NASA TECHNICAL MEMORANDUM

NASA TM X-2054

NASA TM X-2054

FORCE-REDUCED SUPERCONDUCTING TOROIDAL MAGNET COILS

by
Roger W. Boom
Atomics International
and
James C. Laurence
Lewis Research Center

NATIONAL AERONAUTICS AND SPACE ADMINISTRATION • WASHINGTON, D. C. • JULY 1970

1. Report No. NASA TM X-2054	2. Government Accession No.	3. Recipient's Catalog No.
4. Title and Subtitle FORCE-REDUCED SUPERCONDUCTING TOROIDAL MAGNET COILS		5. Report Date July 1970 6. Performing Organization Code
7. Author(s) Roger W. Boom, Atomics International; and James C. Laurence, Lewis Research Center		8. Performing Organization Report No. E-5085
9. Performing Organization Name and Address Lewis Research Center National Aeronautics and Space Administration Cleveland, Ohio 44135		10. Work Unit No. 129-02 11. Contract or Grant No. 13. Type of Report and Period Covered Technical Memorandum
12. Sponsoring Agency Name and Address National Aeronautics and Space Administration Washington, D.C. 20546		14. Sponsoring Agency Code

15. Supplementary Notes

16. Abstract

Two force-reduced toroids have been built with copper-plated niobium-zirconium superconductor wire. The dimensions of the toroids are 30.5 cm major diameter and 3.2 cm minor diameter. The design goal was that each wire should be in a field longitudinal to within $\pm 15^{\circ}$. The objective was to determine if advantage can be gained from the unusually high current capacity of a common type II superconductor in longitudinal fields for the design of magnets. The result found is that a force-reduced toroid of 0.025-cm-diameter niobium - 25-percent-zirconium wire will carry 63 A. This current is to be compared with the usual 18 to 20 A current carried by solenoids built with similar wire. The results are also to be compared with short sample critical currents of ~176 A for the same wire in longitudinal fields. Preliminary reports of these magnets have been presented. A smaller toroid, 30.5 cm major diameter and 2 cm minor diameter, constructed in a similar fashion carried a maximum of 62 A.

17. Key Words (Suggested by Author(s))	18. Distribution Statement
Superconductivity Force-reduced toroids Magnets	Unclassified - unlimited

19. Security Classif. (of this report)	20. Security Classif. (of this page)	21. No. of Pages	22. Price*
Unclassified	Unclassified	28	$3.00

*For sale by the Clearinghouse for Federal Scientific and Technical Information
Springfield, Virginia 22151

FORCE-REDUCED SUPERCONDUCTING TOROIDAL MAGNET COILS*

by Roger W. Boom† and James C. Laurence

Lewis Research Center

SUMMARY

Two force-reduced toroids have been built with copper-plated niobium-zirconium superconductor wire. The dimensions of the toroids are 30.5-centimeter major diameter and 3.2-centimeter minor diameter. The design goal was that each wire should be in a field longitudinal to within $\pm 15^{\circ}$. The objective was to determine if advantage can be gained from the unusually high current capacity of a common type II superconductor in longitudinal fields for the design of magnets. The result found is that a force-reduced toroid of 0.025-centimeter-diameter niobium - 25-percent-zirconium wire will carry 63 amperes. This current is to be compared with the usual 18- to 20-ampere solenoids built with similar wire. The results are also to be compared with short sample critical currents of approximately 176 amperes for the same wire in longitudinal fields. Preliminary reports of these magnets have been presented. A smaller toroid, 30.5-centimeter major diameter and 2-centimeter minor diameter, constructed in a similar fashion carried a maximum of 62 amperes.

INTRODUCTION

Force-free magnets have long been considered as a means for overcoming strength of material limitations for high magnetic fields. Cockcroft (ref. 1) and Kapitza (ref. 2) in the 1920's constructed magnets with more uniform hydrostatic pressures throughout the conductor region. More recently, groups at Princeton (refs. 3 and 4), MIT (ref. 5), and Livermore (ref. 5) have designed a variety of copper magnets in force reduced configurations. Usually the goal was to achieve high pulsed fields without destroying the magnets (copper flows in the usual 50 T solenoid), with a minimum of mechanical sup-

*Work done under NASA contract NAS 3-7867.

†Atomics International, Canoga Park, California, presently at Nuclear Engineering Department and Instrumentation Systems Center, University of Wisconsin, Madison, Wisconsin.

port. In some cases this was accomplished by translating pressures from a small to a large force-bearing surface.

It can be shown that only infinite structures are truly force free. This was most directly demonstrated by Spitzer (ref. 5) with the following equation:

$$\int_{\text{Space}} \bar{r} \cdot (\bar{i} \times \bar{H}) dv = \int_{\text{Space}} E_m \, dv$$

which is positive unless E_m, the magnetic energy density, is not identically zero. (Symbols are defined in appendix A.) In the same view, Levy (ref. 6) has shown that any magnet producing a field must be held together with a structural mass proportional to the stored energy.

The basic idea involved in force-free magnets is that conductors which are parallel to a magnetic field experience no forces since

$$\bar{j} \times \bar{B} = 0$$

The design of such a magnet is simply an attempt to reduce $\bar{j} \times \bar{B}$ everywhere. The two general design methods employed have been to use computing codes and analog methods for the analytically insoluble equations. In the first, a conductor configuration is assumed, the field is computed, and an iterative process brings fields and currents partially into alinement. In the second, the equations are transformed to resistive network analogs (resistors or electrolytic tanks) with subsequent trial and error solutions. Both methods represent a substantial effort and were not used for our initial experiments. In brief, two magnets were designed by means of an approximate solution to the equations. Magnets were built according to this design and were tested. Enhanced current capacity for Nb-Zr superconducting wire was obtained for these magnets.

SUPERCONDUCTIVITY AND FORCE-FREE CONFIGURATIONS

In addition to structural simplicity and weight reductions, the use of force-free superconductor toroids offers exciting possibilities regarding current capacity. Measurements at all laboratories have shown that superconductors carry more current in longitudinal fields than in transverse fields. The first measurements on niobium-zirconium (Nb-Zr) by Sekula, Boom, and Bergeron (ref. 7), Oak Ridge, are shown in figure 1. The 0.025-centimeter Nb-Zr wire is shown to carry up to 400 amperes at 3.0 teslas (30 kG). Figure 2 shows results for tantalum-titanium (Ta-Ti) and molybdenum-rhenium (Mo-Re) (ref. 7). It seems to be true that short sample tests show peaks in the longitudinal (I, H) curves for any material tested. Bergeron (ref. 8)

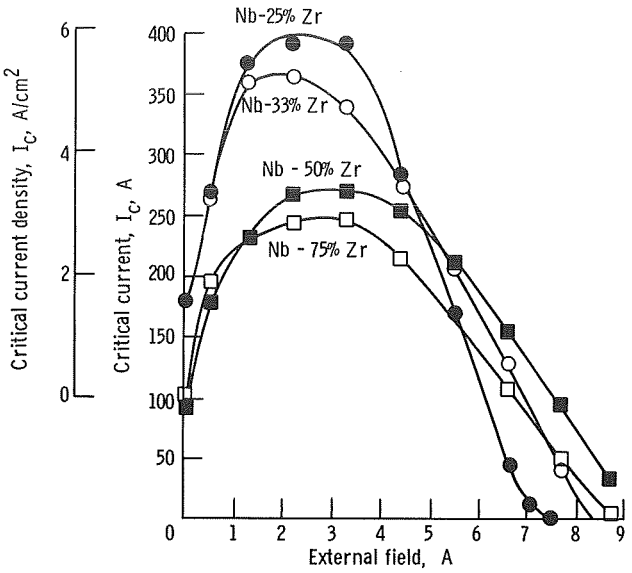

Figure 1. - Longitudinal critical current as function of applied field for several cold-drawn Nb-Zr alloys. Longitudinal field; temperature, 4.2 K; 0.025-centimeter-diameter, 5-centimeter long samples.

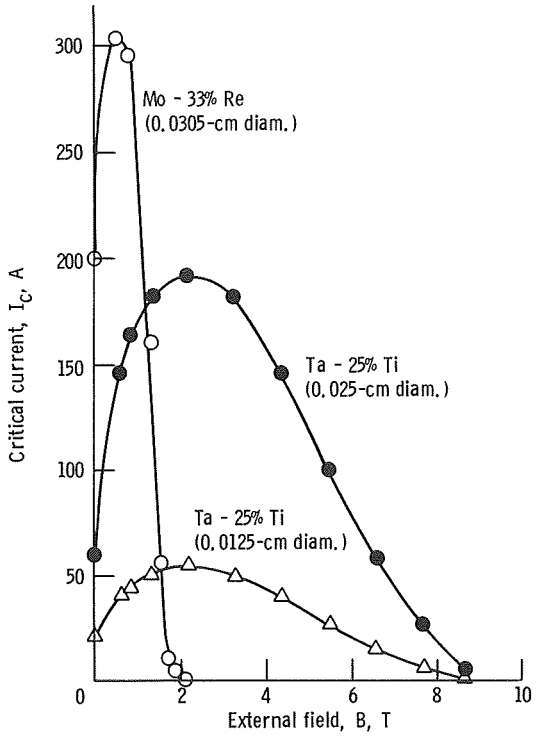

Figure 2. - Longitudinal critical current as function of applied field for cold-drawn Ta - 25-percent-Ti and Mo - 33-percent-Re samples. Longitudinal field; temperature, 4.2 K.

has given plausibility arguments to show that current conduction in a wire itself may favor force-free flow.

More recent measurements reported in reference 7 are given in figure 3. These data show that enhanced currents are expected for moderately large angles between current and field. As applied to magnets this means that high currents should be expected even for the practical magnet in which mechanical and theoretical imperfections are present.

The only force-free magnet known to have been constructed prior to the ones described herein is that reported in reference 7. A small one-layer Nb-Zr toroid with a 10-centimeter inside diameter and 1.27-centimeter cross section carried 120 amperes and produced a longitudinal field of about 0.4 tesla (4 kG) at the windings. Although the current is large compared to the usual 20-ampere magnet current, it must be evaluated conservatively since only 46 meters of wire was used.

The benefits accruing to the superconducting magnets carrying larger currents are obvious, since the field produced is proportional to current, a factor of 10 increase in current capacity, for example, means that only 1/10 the amount of wire is required. As energy storage devices, the advantages of superconducting magnets are even more striking; $1/2\ LI^2$ increases as the square of the current.

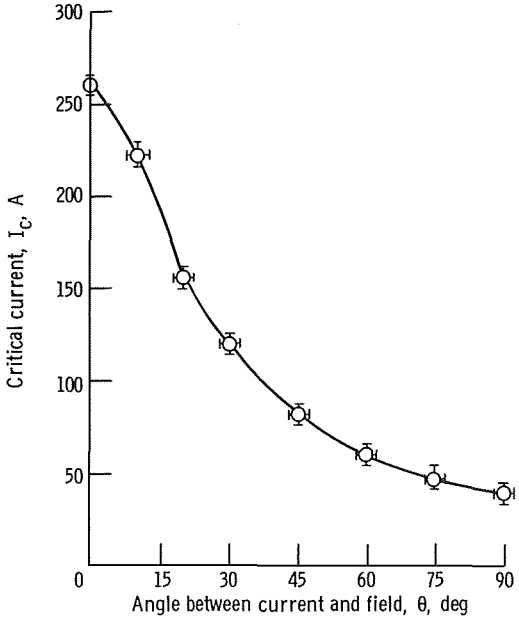

Figure 3. - Critical current as function of angle in external field. Temperature, 4.2 K; magnetic field, 30 kilogauss; 0.025-centimeter-diameter Nb - 33-percent-Zr wire.

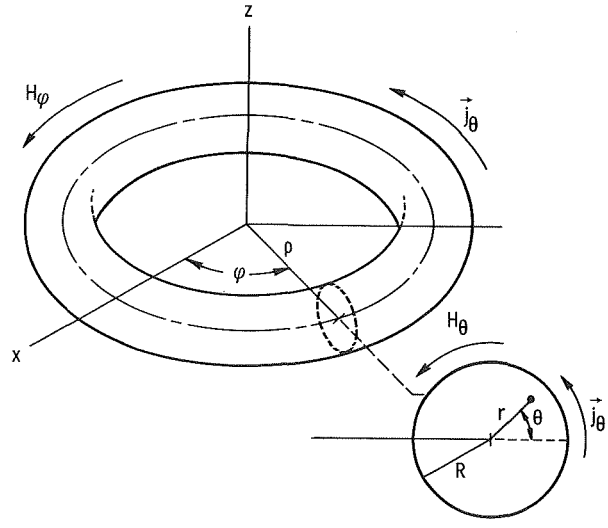

Figure 4. - Schematic of toroid currents.

As mentioned previously, two magnets based on an approximate solution were built. The approximate solution is outlined as follows (ref. 9):

For the toroid shown in figure 4

$$\bar{j} = \bar{j}_\theta + \bar{j}_\varphi \tag{1}$$

and

$$\oint_u \bar{H}_\varphi \cdot \overline{dl} = \int_r^R j_\theta 2\pi\rho \, dr \tag{2}$$

where $u = \rho + r \cos \theta$

$$\oint_r \bar{H}_\theta \cdot \overline{dl} = \int_0^r j_\varphi 2\pi r \, dr \tag{3}$$

An analogy may be made to the infinite solenoid discussed in appendix B, if it is assumed that

$$\left.\begin{aligned} j_\theta &= c\alpha J_1(\alpha r) \\ j_\varphi &= c\alpha J_0(\alpha r) \end{aligned}\right\} \quad \text{at} \quad \theta = 90^\circ \tag{4}$$

with

$$\alpha R \simeq 2.4 \text{ (first zero of } J_0(x))$$

$$\alpha = \text{Constant}$$

$$\bar{j} = \alpha \bar{H}$$

$$c = \text{Strength function, } \frac{\text{ampere turns}}{\text{meter}}$$

If these values are inserted in equations (2) and (3),

$$H_{\varphi} = \frac{\rho}{\rho + r \cos \theta} cJ_0(\alpha r) \tag{5}$$

$$H_{\theta, av} = cJ_1(\alpha r) \tag{6}$$

For $\rho > r$ we see by comparison with the infinite solenoid solution given in appendix B that

$$H_{\varphi} \rightarrow cJ_0(\alpha r) = \frac{j_{\varphi}}{\alpha} \tag{7}$$

$$H_{\theta, av} \rightarrow cJ_1(\alpha r) = \frac{j_{\theta}}{\alpha} \tag{8}$$

which are the statements of the force-free condition. For finite r and ρ the errors in magnitude for H are of the order $(\Delta H/H) \sim (r/\rho)$.

Although not specifically evaluated, both H_{θ} and H_{φ} are larger on the inner diameter and smaller on the outer than predicted in equations (7) and (8) so that the pitch angle error is smaller than that predicted by equation (5). Both components of current densities are also higher on the inner diameter, tend to reproduce the predicted pitch angle, and reduce the error in α.

TOROID CONSTRUCTION

The central turns were wound in a thin wall stainless tube in the form of a hoop and epoxied in place. The winding skeleton for a toroid was thus a 30.5-centimeter-diameter hoop in which there were 63 wires epoxied within a 0.5-centimeter-diameter cross section. Each succeeding layer was wound at a spiral pitch angle given by

$$\tan \gamma = \frac{j_{\varphi}}{j_{\theta}} = \frac{J_0(\alpha r)}{J_1(\alpha r)} \tag{9}$$

where φ is the coordinate along the major circumference and θ is an angle around the minor circumference.

The gross current density was adjusted to the requirement that

$$j = \sqrt{j_\varphi^2 + j_\theta^2} = c\alpha\sqrt{J_0^2(\alpha r) + J_1^2(\alpha r)} \tag{10}$$

by varying the wire density per layer. In that way, a toroid could be a one wire magnet operated with all layers in series. The cross section was divided into seven sections with average pitch angles of 0°, $22\frac{1}{2}^\circ$, 36°, 48°, 60°, 72°, and 90°. All wires were laid down with $\pm 15^\circ$ from the winding prescription (eq. (9)). As constructed, the toroid was 30.5 centimeters in mean diameter with a final layer wire center minor diameter of 3.1 centimeters. For this case,

$$\alpha = \frac{156}{m}$$

$$c = I \times 2\times 10^4 \ \text{A/m}^2 \tag{11}$$

Winding parameters are listed in table I, and a toroid winding is sketched in figure 5. Table II established machine winding speeds and wire densities, and table III compares goals with achieved sizes and wire densities. Values for both toroids 1 and 2 are given in table III.

TABLE I. - TOROID SUBDIVISIONS

Section	Inner radius, r_i, cm	Outer radius, r_0, cm	Angle span, deg	Winding angle, γ, deg	$\sin\gamma$	$\tan\gamma$	Area, cm^2 (a)	Current density, j_φ, required (b)	Wire ends required (c)
I	0	0.25	90 to 78	90	1	∞	0.199	1	68
II	.25	.48	78 to 66	72	.951	3.078	.531	.9032	174
III	.48	.69	66 to 54	60	.866	1.732	.743	.7652	226
IV	.69	.90	54 to 42	48	.743	1.11	1.063	.6043	295
V	.90	1.05	42 to 30	36	.588	.7265	.935	.4325	236
VI	1.05	1.24	30 to 15	$22\frac{1}{2}$	.383	.414	1.31	.2470	290
VII	1.24	1.40	15 to 0	0	0	0	1.39	[d].5484	[e]30.0

[a] Area $= \pi\left(r_0^2 - r_i^2\right)$.

[b] $j_\varphi = J_0(\alpha r)$, zero order Bessel function; actual current density = $(3.43\times 10^4\ \text{A/cm}^2)$ (j_φ required).

[c] $c_W = \dfrac{j_\varphi \pi\left(r_0^2 - r_i^2\right)}{I \sin\gamma}$; I = 100 A.

[d] j_φ required = j_θ.

[e] Per linear cm.

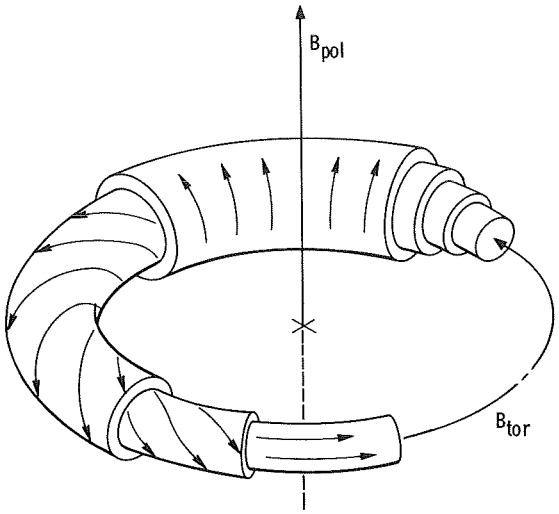

Figure 5. - Partially force-free multilayer toroid. Four layers shown; arrows indicate current direction.

Sections II to VI were initially planned to have four layers each. However, as shown in table III, sections III and V only have three layers, because of the lack of space. For those two sections it was possible to wind more turns per layer so that less than 5 percent of the turns were lost. The sixth section was 14 percent low in gross current density because of an unavoidable geometric constraint. The angle for winding section VI is such that too few turns can be made even though four layers were achieved. The relative rotation speed (turns of wire per revolution of the hoop) given in table III is only approximate since the final criterion is that an even number of equally spaced turns must be wound on each surface. This requirement proved to be more stringent than was possible to design into the machine, so that final operator measurement and adjustment were required, particularly for the first few transverses per layer. The columns in table III labeled wires per cross section give the number of traverses per section which must satisfy equations (9) to (11). After the central section is wound, all succeeding section wire densities as well as the section radial dimensions are fixed. Figure 5 is a sketch of four typical layers which indicates the overall winding directions for the inner, the outer, and two intermediate layers.

The variable pitch toroid winder is shown in figure 6. The wire spool is rotated through the center of the toroid as shown in figure 7 to make a wrap around the toroid windings. Pitch angles are set by the relative speeds of the toroid and wire spool drives. The two drives are linked, continuously variable, and reversible and have very little backlash. Winding requirements are best described as follows: One traverse on layer 1 of section IV, for example, requires 19 turns at a spiral pitch angle of 48^{o} When the next traverse is wound, each turn must be accurately spaced 0.0127 centime-

TABLE II. - INITIAL WINDING DESIGN

Section	Radius to wire center, r_m, cm	Length, $l = 2\pi \sum r_m$, cm	Difference between wires in a layer, cm	Number of wires, $W = \frac{l}{\frac{0.016}{\sin \gamma} + \Delta}$	W required	Winding surface diameter, cm	W wire end (actual)	Relative speed
I	-----	----	-----	---	68	-----	----	----
II	0.285	9.00	0.010	174	174	0.593	34.5	16.9
	.336					.645	40.5	14.4
	.387					.748	46.5	12.6
	.437					.847	52.5	11.1
III	0.502	14.6	0.018	226	226	1.96	49.3	17.6
	.556					1.06	54.1	15.9
	.607					1.16	59	14.6
	.658					1.27	64	13.5
IV	0.710	19.7	0.013	295	295	1.37	66.5	19.5
	.760					1.47	71.5	18.2
	.810					1.57	76	17.0
	.860					1.66	81	16.0
V	0.922	18.3	0.076	239	236	1.80	74.5	22.8
	.970					1.90	78.5	21.6
	1.020					1.99	83	20.5
VI	1.07	28.2	-----	252	290	2.09	59	35.3
	1.12					2.19	61.5	33.7
	1.17						64	32.4
	1.22					2.40	67	31.1
[a]VII	1.27	-----	-----	---	[b]30/cm	2.50	[b]15.8/cm	----
	1.33					2.62	[b]15.8/cm	----

[a]Current density, j_θ, 1.88×10^4 A/cm^2; current/length, I, 3000 A/cm.

[b]Section VII was wound at 90° pitch angle and is best described by turns per cm.

TABLE III. - WINDING PARAMETERS

Section	Average winding angle, γ, deg	Subsection winding surface diameter, cm		Relative rotation speed (approx.)	Wires per cross section		
		Toroid 1	Toroid 2		Planned	Toroid 1	Toroid 2
I	90	-----	-----	----	---	----	----
II	72	0.550	0.558	16.6	68	63	63
		.687	.687	13.4			
		.773	.751	12.1	174	174	174
		.980	.980	9.6			
III	60	1.18	1.18	15.7	226	207	207
		1.22	1.22	14.0			
		1.36	1.36	12.5			
IV	48	1.47	1.47	18.2	295	327	325
		1.57	1.57	17.0			
		1.71	1.71	15.6			
		1.82	1.85	14.6			
V	36	1.97	1.97	20.8	236	246	246
		2.04	2.10	19.8			
		2.18	2.25	18.7			
VI	$22\frac{1}{2}$	2.38	2.34	32.0	290	250	247
		2.46	2.48	30.0			
		2.57	2.62	28.6			
		2.70	2.47	27.4			
VII	0	2.84	2.87	One layer close packed	30/cm	3230	3225
		3.02	3.06	One layer close packed			

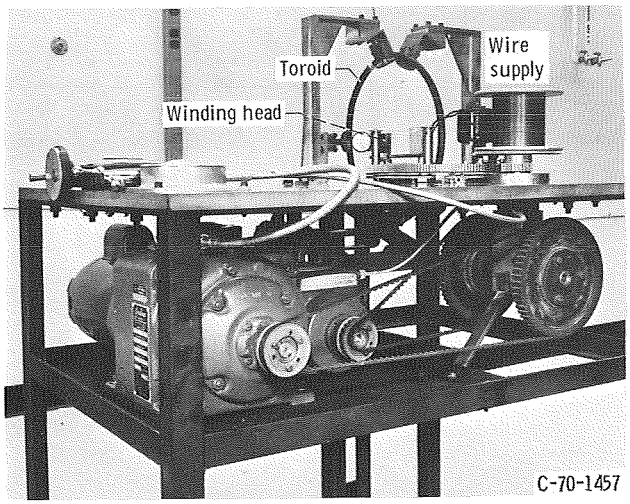

Figure 6. - Variable pitch winder.

Figure 7. - Coil winding.

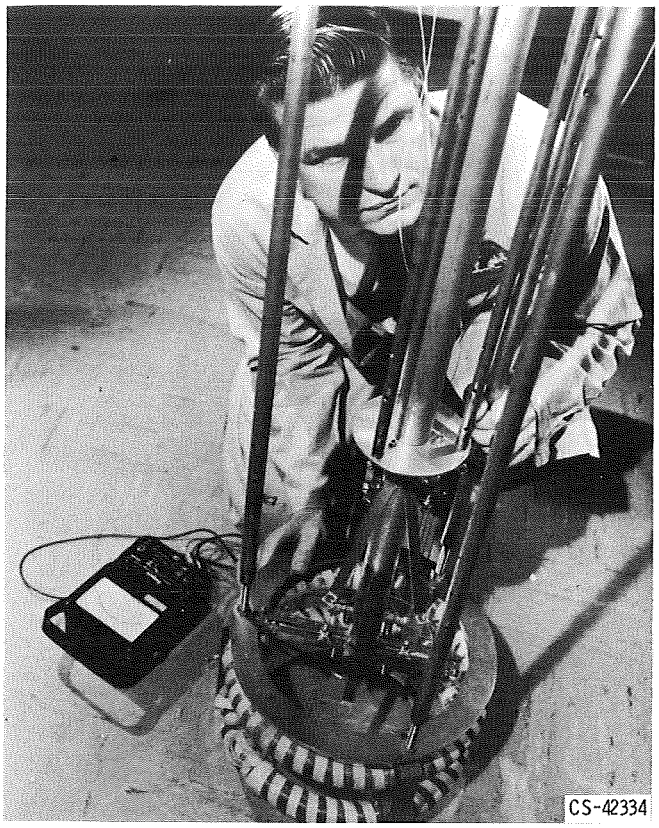

Figure 8. - Two toroids mounted for testing.

ter from each previous turn; all this after traversing the earlier set of windings around a 30.5-centimeter hoop 1.47 centimeter in cross section. The 48^{o} section was one of the easier sections; for others, the spacing dropped to 0.0025 centimeter after winding around a small core on a 95.2-centimeter circumference.

The first spiral layer was wound on a 0.5-centimeter hoop 30.5 centimeter diameter. The outer layer was wound on a 3.0-centimeter-diameter surface. In all, 20 layers were added to the central core. Each layer was epoxied with Emerson and Cuming Stycast 2850 FT. Winding surfaces were brought to dimension by adding layers of epoxy impregnated Nylon mesh and by filing away excess. The two toroids mounted for testing (runs 10 and 11) are shown in figure 8. The starting end was brought out by back-winding a few turns each layer. The main concern throughout was to avoid having any length of wire nonlongitudinal. The leads were spiraled out and away from the toroid so that the copper leads and not the superconductor were in a transverse field.

The conductor was 0.025-centimeter Supercon Nb-25Zr wire, 0.030 centimeter wire with copper plating, and 0.041-centimeter-diameter wire with Nylon insulation. The short sample current at various angles between I and H is given in table IV. Note

TABLE IV. - CRITICAL CURRENT AND MAGNETIC FIELD FOR VARIOUS ANGLES IN EXTERNAL FIELD

[0.025-cm Nb - 25% Zr wire; i_c at zero field, 180 A.]

Angle between current and field, θ, deg	Magnetic field, B, T				
	0.5	1.0	1.5	2.0	2.5
	Critical current, i_c, A				
0	236	240	184	360	240
10	271	200	176	210	230
20	256	232	216	255	240
30	216	240	240	188	210
40	---	---	---	156	144
45	184	155	160	---	---
60	144	96	80	80	76
90	104	64	56	52	49

that the critical currents at all fields indicate peaks in longitudinal fields, with considerable enhancement over the zero field value. The wide scatter in points is due to training effects, which often result in unsatisfactory measurements for such high current densities. These values are used here only as a general comparison with toroid critical current capacities.

RESULTS AND DISCUSSION

Critical currents (see ref. 10) were measured in the two toroids separately, table V, and in both cases the toroids were similar in current carrying capacity (runs 1 to 9). Maximum currents greater than 60 amperes were reached in both. After training to 50 amperes extra copper coated superconductor wire was added at the joints (runs 25 to 46), the input leads were paralleled with a 4000 ampere stabilized cable (runs 47 to 64), and the charging voltage was increased to 10 volts. These changes brought the current level to more than 60 amperes. When operated in series and separated by 5 centimeters (runs 10 and 11), the maximum current was only about 19.5 amperes, which is nonconclusive evidence that lower current levels result when near force-free conditions are destroyed. An alternative explanation is the "split coil effect," which results from an electromechanical interaction which induces instabilities at low current

TABLE V. - TOROID CRITICAL CURRENTS

Toroid	Run	Critical current, I_c, A	Comments	Toroid	Run	Critical current, I_c, A	Comments
2	1	27	Toroids 1 and 2 mounted 6.3 cm apart; only toroid 2 energized	1	32	26	Extra copper coated superconductor wire added at joints
	2	28			33	40	
	3	31			34	41	
	4	34.5			35	38	
					36	34	
1	5	36	Toroids 1 and 2 mounted 6.3 cm apart; only toroid 1 energized; toroid 2 open and/or shorted without effect		37	34	
	6	26			38	42	
	7	36			39	46	
	8	36			40	49	
	9	36			41	50.5	
1 and 2	10	19.5	Toroids in series		42	55	
	11	16	Toroids in series but reversed from run 10		43	57	
					44	56	
1	12	30	Toroid 2 removed, training sequence for toroid 1 alone		45	42	
	13	31			46	24	
	14	30.5					
	15	47		1	47	40	Paralleled input leads with stabilized cable (rated at 4000 A at zero field)
	16	47			48	48	
	17	30			49	52	
	18	27			50	52	
	19	36			51	52	
	20	42			52	53	
	21	30			53	54	
	22	34			54	46	
	23	36			55	48	
	24	50			56	30	
					57	54	
1	25	24	Extra copper coated superconductor wire added at joints		58	38	
	26	32					
	27	32		1	59	52	Charging voltage increased to about 10-V step function
	28	34			60	56	
	29	30			61	55	
	30	34			62	56	
	31	38			63	55	
					64	63	

levels. The experiments do not differentiate but suggest that the force-free conditions are important since most "split coils" limit at lower currents still.

The decay time was about 50 milliseconds, determined primarily by a shorted four-layer external secondary of copper wire (15 ppm impurities), 0.05 centimeter in diameter. The wire is bare and line soldered at each layer around the inside. Sixty-four normal excursions by toroid 1 resulted in no deterioration.

Field measurements in the median plane and around the surfaces of the windings were in moderate agreement with the field calculated for an infinite solenoid. The field on the median plane was measured at room temperature with low current in toroid 1. To compensate for the Earth's field, two sets of readings were obtained with currents reversed and are subtracted from each other. Toroid 2 was checked for general agreement at several points. The results for toroid 1 are shown in table VI.

TABLE VI. - FIELD CALIBRATION FOR TOROID 1 MEASURED IN MEDIAN PLANE

Distance from center, r, cm	Forward current		Reverse current		Difference between forward and reverse current values		Field/current, G/A
	Current, i, A	Magnetic field, B, T	Current, i, A	Magnetic field, B, T	Current, i, A	Magnetic field, B, T	
0	0.0302	2.01×10^{-4}	0.0150	1.15×10^{-4}	0.0152	0.86×10^{-4}	56.6
2.5	.0303	2.05	.0153	1.19	.0150	.86	57.5
3.8	.0304	2.10	.0150	1.20	.0154	.90	58.5
5.1	.0304	2.18	.0150	1.24	.0154	.94	61.0
6.3	.0307	2.32	.0149	1.29	.0158	1.03	65.0
7.6	.0307	2.46	.0153	1.40	.0154	1.06	69.0
8.8	.0306	2.69	.0150	1.50	.0156	1.19	76.1
10.1	.0304	3.18	.0153	1.72	.0151	1.46	96.9
11.4	.0306	3.75	.0156	2.10	.0150	1.65	110.0
12.7	.0306	5.20	.0155	2.76	.0151	2.44	161.0

TABLE VII. - FIELDS IN MEDIAN PLANE

OUTSIDE TOROID 1

[X measured from toroid surface.]

Distance from toroid surface, X, cm	Field/current, T/A	Distance from toroid surface, X, cm	Field/current, T/A
0	92×10^{-4}	3.18	29×10^{-4}
.64	71	3.81	25
1.27	55	4.55	21
1.90	44	5.10	19
2.54	35	5.74	17

Fields were also measured on the median plane outside the magnet. If X is the distance from the toroid surface, then, at room temperature the measured fields are those given in table VII. Table VIII presents the fields measured at low temperature for toroid 1 carrying 20 amperes.

Table IX presents the fields near the windings and perpendicular to the median plane.

In checking the various tables for consistency, we see that there is no basic disagreement between room temperature and low temperature readings. The important point is that no shorts or unexplained field deviations occurred.

The measurements near the surface show 160×10^{-4} tesla per ampere inside on the median plane. At 63 amperes this field is 1 tesla. The outer layer of Nb-Zr has been covered with epoxy and with four layers of 0.05-centimeter copper (the protective sec-

TABLE VIII. - FIELD IN MEDIAN PLANE

[Temperature, 4.2 K; current, 20 A.]

Distance from center, r, cm	Hall voltage (at 100 mA Hall current), mV	Current, i, A	Magnetic field, B, T	Field/current, T/A
1.27	4.0	20	0.12	60×10^{-4}
2.54	4.5	20	.13	65
10.1	10.0	20	.20	100
12.7	20.0	20	.31	155

TABLE IX. - FIELD NEAR WINDINGS, AT 90° TO MEDIAN PLANE

[X measured from toroid surface.]

Distance from toroid surface, X, cm	Hall voltage (at 100 mA Hall current), mV	Current, i, A	Magnetic field, B, T	Field/current, T/A
0	23	20	0.33	165×10^{-4}
2.54	7	20	.16	80
5.1	4	20	.12	60
7.6	2.8	20	.10	50

ondary). The Nb-Zr surface field extrapolates to about 190×10^{-4} tesla per ampere.

Two sources of differences between an idealized calculation and actual toroid performance will be considered: first, the error in pitch winding angle, and second, the approximation which results from using calculated winding parameters as a comparison between measured and calculated fields. Errors in pitch winding come from three causes: first, the winding volume is divided into seven sections with the winding pitch angle γ constant in each section. The sections are chosen so that $\Delta\gamma < \pm 7.5^{\circ}$. Second, in wrapping a spiral turn around a toroid core, the pitch angle is greater on the outer surface than on the inner surface because of different radii of curvature. This can be expressed as

$$\frac{\Delta(\tan \gamma)}{\tan \gamma} < \frac{2r}{R}$$

where r/R is the ratio of major to minor radii per layer. The resulting error is

r/R	$\Delta\gamma$, deg
0	0
.5	.8
.6	1.5
.8	5.5
1.0	5

Third, errors occur because of excess or insufficient turns per section, provided wire crowding is the cause. This error is of significance only in section VI. The angle span for that section was larger than that for earlier sections (15°), and 250 turns were achieved instead of the desired 290. However, by overwinding the previous sections, only a net number of 20 turns was lost. This error was ignored since the loss is only 20 turns in about 1000.

To summarize, if wire crowding errors are neglected,

$$\Delta\gamma < 7.5^{\circ} + 5^{\circ} = 12.5^{\circ}$$

Referring to table IV, an error of this amount in γ implies that the short sample current capacity is greater than 170 amperes.

Before a true comparison of the measured and calculated fields can be made, the fields should be recalculated based on the winding actually achieved. Thus:

$$R = 1.54 \text{ cm}$$

$$\alpha = \frac{2.4}{0.0154} = 156$$

$$j_{\varphi,0} = \left(\frac{63 \text{ wires actual}}{69 \text{ wires planned}}\right)\left(3.43\times10^{4}\ \frac{A}{m^2}\right)$$

$$j_{\varphi,0} = 3.12\times10^{8}\ \frac{A}{m^2} \quad \text{at } 100 \text{ A}$$

$$B_{\varphi,0} = \mu_0 H_{\varphi,0} = \frac{3.12\times10^{8}\ \mu_0}{156} = 2\times10^{6} \times 4\pi\times10^{-7},\ \text{T}$$

$$B_{\varphi,0} = 2.5 \text{ T}$$

Hence,

$$\frac{B_{\varphi,0}}{I_{\varphi,0}} = \frac{2.5000 \text{ T}}{100 \text{ A}}$$

$$= 0.0250\ \frac{T}{A}$$

On the surface of an infinite solenoid

$$B_{\text{surface}} = 0.52\ B_{\varphi,0}$$

$$= \left(0.025\ \frac{T}{A}\right)(0.52)$$

$$= 0.0130\ \frac{T}{A}$$

Because the magnet is a toroid, we should expect the field correction to be $(\Delta H/H) \simeq (R/\rho) = 10$ percent, that is, 10 percent high inside and 10 percent low outside. From the tabulated values at the surface of the toroid, we have

$$B_{\varphi,\,\text{surface}} = 92 + 10\% \simeq 0.01\,\frac{T}{A}\ \text{outside}$$

$$= 165 - 10\% \simeq 0.015\,\frac{T}{A}\ \text{inside}$$

$$= 155 \pm 10\% \simeq 0.0155\,\frac{T}{A}\ \text{top}$$

while $B_{\text{calculated}} = 0.0130$ T/A. The discrepancy seems largest outside, which is perhaps reasonable since the external field falloff is the most rapid. A more careful force-free computation might increase the approximate 10 percent correction applied, and the higher correction would lead to better agreement between the measured-adjusted values and the calculated values.

The field variation within the windings is given by

$$H = c\sqrt{J_0^2(\alpha r) + J_1^2(\alpha r)}$$

The calculated central field at 63 amperes is 1.6 teslas at an overall central current density of 18,000 amperes per square centimeter. The field drops to 0.8 tesla at the surface, subject to the variations and corrections just mentioned.

CONCLUDING REMARKS

The errors in positioning the wires are large but well within the longitudinal tolerances which should yield current enhancement. The maximum current found, 63 amperes, is an intermediate value (above 20 A but below 170 A) which demonstrates that the force-free condition is favorable to higher current levels. Degradation in the performance of the toroids occurs whenever the force-reduced conditions are removed, that is, when another magnet is mounted close by.

Lewis Research Center,
National Aeronautics and Space Administration,
Cleveland, Ohio, May 14, 1970,
129-02.

APPENDIX A

SYMBOLS

B	magnetic field	r	radius (see fig. 4)
c	strength function	v	volume
E_m	energy density	W	number of wires
H	flux density	x, y, z	coordinates (see fig. 4)
I	current/length	α	constant
i	current	γ	pitch angle
$J_0(x)$, $J_1(x)$	Bessel functions	θ	see fig. 4
j	current density	ρ	major radius of toroid (see fig. 4)
L	inductance		
l	length	φ	see fig. 4
R	minor radius of toroid (see fig. 4)		

APPENDIX B

CURRENT-FIELD RELATIONS FOR AN INFINITE SOLENOID

Consider the infinite solenoid (fig. 9). There are only two components of current in this solenoid, $\bar{j}_\theta$ and $\bar{j}_z$. To the basic equations

$$\nabla \times \bar{H} = \bar{j} \tag{B1}$$

$$\nabla \cdot \bar{B} = 0 \tag{B2}$$

$$\nabla \cdot \bar{j} = 0 \tag{B3}$$

is added the force-free condition

$$j = \alpha \bar{H} \tag{B4}$$

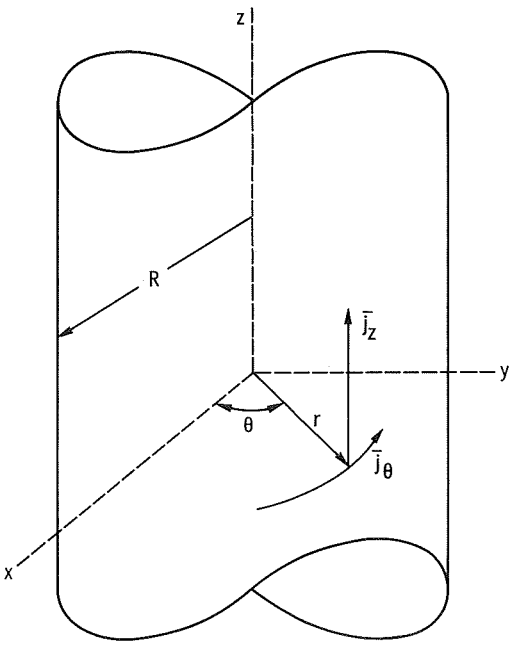

Figure 9. - Schematic of infinite solenoid.

with α constant. The well-known solution in Bessel functions may be outlined as follows. In Cartesian coordinates, equations (B1) and (B4) become

$$\bar{e}_x\left(\frac{\partial H_z}{\partial y} - \frac{\partial H_y}{\partial z}\right) + \bar{e}_y\left(\frac{\partial H_x}{\partial z} - \frac{\partial H_z}{\partial x}\right) + \bar{e}_z\left(\frac{\partial H_y}{\partial x} - \frac{\partial H_x}{\partial y}\right) = \bar{e}_x \alpha H_x + \bar{e}_y \alpha H_y + \bar{e}_z \alpha H_z \tag{B5}$$

With α constant and the solenoid infinitely long, all components of H are independent of z. Therefore

$$\bar{e}_x\left(\frac{\partial H_z}{\partial y}\right) + \bar{e}_y\left(-\frac{\partial H_z}{\partial x}\right) + \bar{e}_z\left(\frac{\partial H_y}{\partial x} - \frac{\partial H_x}{\partial y}\right) = \bar{e}_x \alpha H_x + \bar{e}_y \alpha H_y + \bar{e}_z \alpha H_z \tag{B6}$$

$$\frac{\partial H_z}{\partial y} = \alpha H_z \tag{B7}$$

$$-\frac{\partial H_z}{\partial x} = \alpha H_y \tag{B8}$$

$$\frac{\partial H_y}{\partial x} - \frac{\partial H_x}{\partial y} = \alpha H_z \tag{B9}$$

From equation (B8)

$$\frac{\partial^2 H_z}{\partial x^2} = -\alpha \frac{\partial H_y}{\partial x} \tag{B10}$$

From equation (B7)

$$\frac{\partial^2 H_z}{\partial y^2} = \alpha \frac{\partial H_x}{\partial y} \tag{B11}$$

and

$$\frac{\partial^2 H_z}{\partial z^2} = 0 \tag{B12}$$

Adding gives

$$\nabla^2 H_z = \alpha\left(\frac{\partial H_x}{\partial y} - \frac{\partial H_y}{\partial x}\right) \tag{B13}$$

and with equation (B9)

$$\nabla^2 H_z + \alpha^2 H_z = 0 \tag{B14}$$

Therefore

$$H_z = cJ_0(\alpha r) \tag{B15}$$

where J_0 is the zero order Bessel function. Next construct the following identity, remembering that $\partial/\partial z = 0$:

$$\nabla H_z \times \bar{e}_z = \bar{e}_x \frac{\partial H_z}{\partial y} - \bar{e}_y \frac{\partial H_z}{\partial x} \tag{B16}$$

If equations (B7) and (B8) are substituted in equation (B16),

$$\nabla H_z \times \bar{e}_z = \bar{e}_x(\alpha H_x) + \bar{e}_y(\alpha H_y) \tag{B17}$$

$$= \alpha \bar{H}_\theta \tag{B18}$$

Thus

$$\bar{H}_\theta = \frac{1}{\alpha} \nabla H_z \times \bar{e}_z \tag{B19}$$

since

$$\nabla H_z \times \bar{e}_z = c\nabla\left[J_0(\alpha r)\right] \times \bar{e}_z \tag{B20}$$

$$= -\bar{e}_\theta c \frac{\partial J_0(\alpha r)}{\partial r} \tag{B21}$$

$$= \bar{e}_\theta c\, \alpha J_1(\alpha r) \tag{B22}$$

Then

$$\bar{H}_\theta = \frac{1}{\alpha} \nabla H_z \times \bar{e}_z = \bar{e}_\theta c J_1(\alpha r) \tag{B23}$$

and

$$\left.\begin{aligned} j_z &= \alpha H_z = c\,\alpha J_0(\alpha r) \\ j_\theta &= \alpha H_\theta = c\,\alpha J_1(\alpha r) \end{aligned}\right\} \tag{B24}$$

Outside the solenoid, $j = 0$ and $\partial/\partial z = 0$, and from equations (B7) to (B8)

$$\nabla H_z = 0 \tag{B25}$$

or

$$H_z = \text{constant to infinity} \tag{B26}$$

Therefore

$$H_z = 0, \qquad r > R \tag{B27}$$

and, in particular, at the boundary $r = R$

$$H_z = 0 = cJ_0(\alpha R) \tag{B28}$$

Thus

$$\alpha R \cong 2.4 \tag{B29}$$

and

$$\alpha = \frac{2.4}{R} \tag{B30}$$

Total current in the z-direction is

$$I_z = c\alpha \int_0^R J_0(\alpha r) 2\pi r \, dr \tag{B31}$$

$$= 2\pi c R J_1(\alpha R) \tag{B32}$$

The circuital equation

$$\oint \overline{H} \cdot \overline{dl} = \sum I = 2\pi c R J_1(\alpha R) \tag{B33}$$

for $r > R$ is

$$H_\theta 2\pi r = 2\pi c R J_1(\alpha R) \tag{B34}$$

or

$$H_\theta = c \frac{R}{r} J_1(\alpha R) \tag{B35}$$

The following complete solution for a solenoid of radius R is shown in figure 10:

$$\left.\begin{aligned} j_z &= \alpha H_z = c\alpha J_0(\alpha r) \\ j_\theta &= \alpha H_\theta = c\alpha J_1(\alpha r) \end{aligned}\right\} \quad r < R \tag{B36}$$

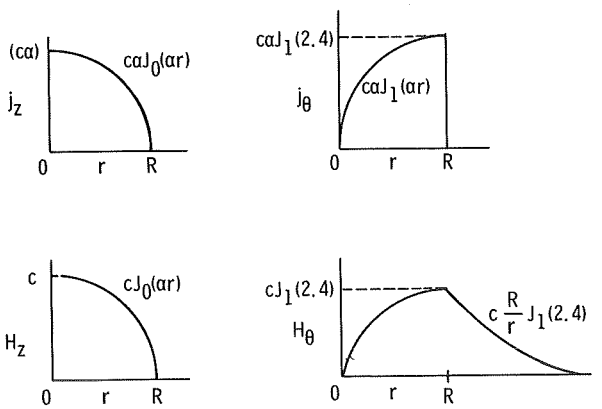

Figure 10. - Current and fields for force-free infinite solenoid.

$$\left.\begin{aligned} j_z &= 0; \qquad H_z = 0 \\ j_\theta &= 0; \qquad H_\theta = c\,\frac{R}{r}\,J_1(\alpha R) \end{aligned}\right\} \quad r > R \tag{B37}$$

$$\left.\begin{aligned} j_z &= \alpha H_z = 0 \\ j_\theta &= \alpha H_\theta = c\,\alpha J_1(\alpha R) \end{aligned}\right\} \quad r = R \tag{B38}$$

where $\alpha R \cong 2.4$, the first zero of $J_0(\alpha R)$.

REFERENCES

1. Cockroft, J. D.: The Design of Coils for the Production of Strong Magnetic Fields. Phil. Trans. Roy. Soc. (London), Ser. A, vol. 227, 1928, pp. 317-343.

2. Kapitza, P.: Method of Obtaining Strong Magnetic Fields. Proc. Roy. Soc. (London), Ser. A, vol. 115, Aug. 1927, pp. 658-683.

3. Wakefield, Kenneth E.: Network Solution of a System Containing a Force-Free Coil and a Force-Bearing Shell. High Magnetic Fields. Henry Kolm, Benjamin Lax, Francis Bitter, and Robert Mills, eds., MIT Press and John Wiley & Sons, Inc., 1962, pp. 39-43.

4. Wells, D. R.; and Mills, R. G.: Force-Reduced Toroidal Systems. High Magnetic Fields. Henry Kolm, Benjamin Lax, Francis Bitter, and Robert Mills, eds., MIT Press and John Wiley & Sons, Inc., 1962, pp. 44-47.

5. Furth, H. P.; Levine, M. A.; and Waniek, R. W.: Production and Use of High Transient Magnetic Fields. II. Rev. Sci. Instr., vol. 28, no. 11, Nov. 1957, pp. 949-958.

6. Levy, Richard H.: Author's Reply to Willinski's Comment on "Radiation Shielding of Space Vehicles by Means of Superconducting Coils." ARS J., vol. 32, no. 5, May 1962, p. 787.

7. Sekula, S. T.; Boom, R. W.; and Bergeron, C. J.: Longitudinal Critical Currents in Cold-Drawn Superconducting Alloys. Appl. Phys. Letters, vol. 2, no. 5, Mar. 1, 1963, pp. 102-104.

8. Bergeron, C. J., Jr.: Simple Model for Longitudinal Force-Free Current Flow in Superconductors of the Second Kind. Appl. Phys. Letters, vol. 3, no. 4, Aug. 15, 1963, pp. 63-66.

9. Van Bladel, J.: Some Remarks on Force-Free Coils. Nucl. Instr. Methods, vol. 16, 1962, pp. 101-112.

10. Laurence, J. C.: Superconductive Magnets at Lewis Research Centre of N. A. S. A. Cryogenic Engineering: Present Status and Future Development. Heywood-Temple Industrial Publ. Ltd., 1968, pp. 94-98.

NATIONAL AERONAUTICS AND SPACE ADMINISTRATION
WASHINGTON, D.C. 20546
OFFICIAL BUSINESS

FIRST CLASS MAIL

POSTAGE AND FEES PAID
NATIONAL AERONAUTICS AND
SPACE ADMINISTRATION

POSTMASTER: If Undeliverable (Section 158 Postal Manual) Do Not Return

"The aeronautical and space activities of the United States shall be conducted so as to contribute . . . to the expansion of human knowledge of phenomena in the atmosphere and space. The Administration shall provide for the widest practicable and appropriate dissemination of information concerning its activities and the results thereof."

— NATIONAL AERONAUTICS AND SPACE ACT OF 1958

NASA SCIENTIFIC AND TECHNICAL PUBLICATIONS

TECHNICAL REPORTS: Scientific and technical information considered important, complete, and a lasting contribution to existing knowledge.

TECHNICAL NOTES: Information less broad in scope but nevertheless of importance as a contribution to existing knowledge.

TECHNICAL MEMORANDUMS: Information receiving limited distribution because of preliminary data, security classification, or other reasons.

CONTRACTOR REPORTS: Scientific and technical information generated under a NASA contract or grant and considered an important contribution to existing knowledge.

TECHNICAL TRANSLATIONS: Information published in a foreign language considered to merit NASA distribution in English.

SPECIAL PUBLICATIONS: Information derived from or of value to NASA activities. Publications include conference proceedings, monographs, data compilations, handbooks, sourcebooks, and special bibliographies.

TECHNOLOGY UTILIZATION PUBLICATIONS: Information on technology used by NASA that may be of particular interest in commercial and other non-aerospace applications. Publications include Tech Briefs, Technology Utilization Reports and Notes, and Technology Surveys.

Details on the availability of these publications may be obtained from:

SCIENTIFIC AND TECHNICAL INFORMATION DIVISION

NATIONAL AERONAUTICS AND SPACE ADMINISTRATION

Washington, D.C. 20546